Moroccan Journal of Chemistry
ISSN : 2351-812X

Mor. J. Chem., 2023, Volume 11, Issue 02, Page 541-552

https://revues.imist.ma/index.php/morjchem

Nucleation and growth mechanism of nickel electrodeposited on ITO substrate in nitrate and chloride electrolytes: Comparative study

Ahmed Sahlaoui[1], Youssef Lghazi[1], Boubaker Youbi[1], Mohammed Ait Himi[1], Jihane Bahar[1], Chaimaa El Haimer[1], Aziz Aynaou[1], Mohamed Ouknin[2], Itto Bimaghra[1], Lhou Majidi[2]*

[1]*Bio-Geosciences and Materials Engineering Laboratory, Higher Normal School, Hassan II University of Casablanca, Casablanca, Morocco.*

[2]*Laboratory of Natural Substances & Synthesis and Molecular Dynamics, Faculty of Sciences and Technics, Moulay Ismail University, 52000 Errachidia, Morocco.*

**Corresponding author, Email address:* *lmajidi@yahoo.fr* or *l.majidi@fste.umi.ac.ma*

Received *12 Jan 2023,*
Revised *23 Mar 2023,*
Accepted *24 Mar 2023*

Citation*: A., Sahlaoui, Y., Lghazi, B., Youbi, M., Ait Himi, J., Bahar, C., El Haimer, A., Aynaou, M., Ouknin, I., Bimaghra, L., Majidi (2023) Nucleation and growth mechanism of nickel electrodeposited on ITO substrate in nitrate and chloride electrolytes: Comparative study, Mor. J. Chem., 11(2), 541-552. Doi: https://doi.org/10.48317/IMIST.PRSM/morjchem-v11i2.36809*

Abstract: In this work, we reported a comparative study of nickel electrodeposition mechanism on indium tin oxide (ITO) from two mediums. The nitrate electrolyte contains 0.01 M of nickel nitrate hexahydrate (Ni $(NO_3)_2$, $6H_2O$) with 0.1M of potassium nitrate (KNO_3) and chloride bath was a mixture of 0.01 M ($NiCl_2$, $6H_2O$) with 0.1 M of potassium chloride (KCl). The electrochemical techniques cyclic voltammetry (CV) and the chronoamperometry (CA) revealed that the electrodeposition of nickel (Ni) at a negative potential around -1.1 V versus SCE (saturated calomel electrode) is quasi-reversible reaction controlled by the diffusion process in the two mediums. The experimental current transient curves are compared to those calculated from Scharifker-Hills models; it was found that the nucleation and growth of Ni on the ITO substrate follows an instantaneous three-dimensional (3D) mechanism in the two solutions, which was confirmed by the micrographs of SEM analysis. The X-ray diffraction characterization of nickel thins films elaborated by chronoamperometry on ITO substrate had shown a cubic crystal structure whatever the electrolyte composition. However, in nitrate solution the formation of a nickel oxide was identified.

Keywords: Nickel; Electrodeposition; Nucleation; Chronoamperometry; Cyclic Voltammetry.

1. Introduction

Thanks to its electrical, magnetic, mechanical, structural and morphological properties, nickel occupies an important place on an industrial scale for applications in catalysis, energy storage and dihydrogen storage, and protection against corrosion (Abbasi-Amandi *et al.,* 2021; Boumezzourh *et al., 2019*; Jamshidi *et al.,* 2018). Nickel can be mass-produced by conventional processes (thousands of tons obtained by pyrrometallurgy and electrolysis) whose control of the structure is not accessible (Chat-Wilk *et al.,* 2021). New physical (PVD) and chemical (CVD) and electrochemical techniques such as electrodeposition have allowed access to nanoscale structures (Sivasakthi *et al.,* 2021). Among these numerous techniques, electrodeposition has received considerable attention as an alternative approach for the production of metallic films. Indeed, the electrodeposition is a less expensive technique, and allows the simple elaboration of metallic films and controls the mechanisms of their

growth (Chat-Wilk *et al.,* 2021). It is also noteworthy that by simply changing the electrodeposition parameters, the properties and characteristics of the deposited films, like nickel coatings, can be modified (Janjan *et al.,* 2011; Deng *et al.,* 2008; El-Hallag *et al.,* 2021; Ibrahim, 2006; Wang *et al.,* 2019). In particular, small variations in bath composition and pH can affect deposit morphology, coating properties and adhesion. These physico-chemical properties are highly dependent upon the mechanism of the early stages of electroplating known as nucleation and growth (Hu *et al.,* 2023; Yue *et al.,* 2022a; Yue *et al.,* 2022b). Various electrolytes are used for the electrodeposition of thin nickel layers such as aqueous solutions, ionic liquids and deep eutectic solvents (DES). In this work, a comparative investigation of the electrochemical deposition of nickel on indium tin oxide (ITO) substrate was carried out using electrochemical techniques in nitrate and chloride electrolytes.

2. Materials and Methods

2.1. Electrodeposition

The electrodeposition of Nickel was studied by cyclic voltammetry (CV) and chronoamperometry (CA) using a three-electrode cell connected to a Versa STAT 3 potentiostat-galvanostat combined with Versa Studio software.

The glass substrate pre-coated with transparent and conducting layers of indium tin oxide (ITO) was used as a working electrode, platinum (Pt) grid was used as the counter electrode and the saturated calomel electrode (SCE) as the reference electrode (all potentials are given relative to this reference).The surface area of the working electrode has been fixed at 1 cm^2. At the beginning of each experiment, the ITO substrate was cleaned in an ultrasonic bath using acetone for 15 minutes, ethanol for 10 minutes and finally with distilled water for 5 minutes.

The electrolyte used is an aqueous solution containing 0.01M nickel nitrate $Ni(NO_3)_2.6H_2O$+ 0.1M potassium nitrate KNO_3 for nitrate medium and 0.01M nickel chloride $NiCl_2.6H_2O$+ 0.1M potassium chloride KCl for chloride medium. All experiments were carried out at a neutral pH (around 7) and ambient temperature (T≈20° C).

2.2. Characterization

The nickel electrodeposited thin films were characterized by X-ray diffraction (XRD) analysis, using a Broker D8 Advance diffractometer, equipped with a graphite monochromator, a Lynx-Eye detector, and parallel beam optics Cu Kα radiation (λ = 1.5411 Å). The surface morphology was investigated using the scanning electron microscopy (SEM) Philips XL30FEG.

3. Results and Discussion

3.1 Cyclic voltammetry

Cyclic Voltammetry (CV) is an electrochemical potentiodynamic technique, which measures the current that develops in an electrochemical cell by cycling the potential of a working electrode, ramped linearly versus time. This technique was also used in order to identify the potential region, the reversibility and the kinetic of redox reactions involved in the nickel electrodeposition.

Firstly; a preliminary study was necessary to investigate the substrate stability on different used mediums; then, the redox systems were identified simultaneously. The figures 1a and b illustrated the obtained result for nickel electrodeposition in nitrate and chloride electrolytes, accompanied by blank solution voltammograms (supporting electrolyte alone), for a scan rate of 20 $mV.s^{-1}$ in the potential window of -0.6 V to -1.5 V vs SCE.

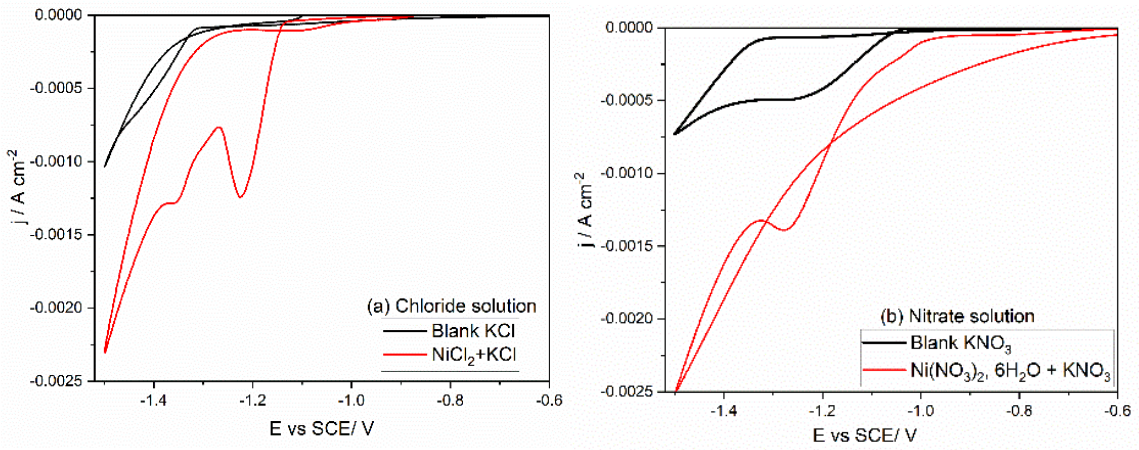

Figure 1. Cyclic voltammograms of Ni electrodeposition on ITO substrate and supporting electrolytes (Blanks) at scan rate 20 mV s^{-1}: (a) from chloride solution and (b) from nitrate solution.

In nitrate and chloride blanks, curves (1) in **Figure 1a** and **b**, we noted, the stability of ITO substrate in all the range potential used, with the absence of any reduction or oxidation peaks of the indium tin oxide substrate. However, the cathodic reduction system observed in both solutions corresponds to water reduction according to **Eqn. 1**, and in nitrate medium, this reduction is accompanied by the nitrate reduction (**Eqn. 2**).

$$H_3O^+ + 1e^- \rightleftharpoons \tfrac{1}{2}\, H_2 + H_2O \qquad \textbf{(Eqn. 1)}$$

$$NO_3^- + H_2O + 2e^- \rightleftharpoons NO_2^- + 2HO^- \qquad \textbf{(Eqn. 2)}$$

The presence of nickel(II) ions in solution is subject to a reduction of one peak at -1.27 V/SCE for the nitrate medium and a reduction two peaks in a chloride medium -1.1 and -1.16 V/SCE, these peaks correspond to the electrodeposition of Nickel on the ITO substrate. According to the literature (Chat-Wilk *et al.,* 2021; Oluranti *et al.,* 2012), the electrodeposition mechanism in chloride medium involves two consecutive one-electron charge transfers with adsorption of intermediary nickel cationic complex as shown in the following equations (3) , (4) and (5) :

$$Ni^{2+} + Cl^- = NiCl^+ \qquad \textbf{(Eqn. 3)}$$

$$NiCl^+ + e^- = NiCl_{ads} \qquad \textbf{(Eqn. 4)}$$

$$NiCl_{ads} + e^- = Ni + Cl^- \qquad \textbf{(Eqn. 5)}$$

Then, the first cathodic pic at -1.1 V vs SCE can be attributed to $NiCl^+$ reduction; it is also followed by the deposition of Ni according to the reaction 4 at the potential -1.16V vs SCE literature (Chat-Wilk *et al.,* 2021; Oluranti *et al.,* 2012).

$$Ni^{2+}(aq) + 2e^- = Ni/ITO \qquad \textbf{(Eqn. 6)}$$

It should be noted that the nickel deposition is very close to the electrochemical solvent wall, it then interferes with the reduction of nitrate and hydrogen ions and this facilitates the formation of oxide or hydroxide by passivation according to equations (7) and (8) (Badea *et al.,* 2010; Ritzert and Moffat 2016).

$$NO_3^-{}_{(aq)} + Ni/ITO + H_2O_{(l)} = Ni(OH)_2 + NO_2^-{}_{(aq)} \qquad \textbf{(Eqn. 7)}$$

$$Ni(OH)_2 = NiO + H_2O_{(l)} \qquad \textbf{(Eqn. 8)}$$

To study the reversibility and the type of control involved during nickel electrodeposition, a series of voltammograms have been recorded for nitrate and chloride solutions in potential range between 0 and -1.5 V/SCE with different scan rates (5, 10, 15, 20 and 25 mV s^{-1}). **Figure 2a** and **b** shows the obtained result. It was found that nickel can be deposited on ITO substrate in two mediums through cathodic reaction and a slight shift in the nickel deposition potential was observed when changing from the chloride medium (started at -1.0 V /SCE) to the nitrate medium (started at -1.1 V /SCE):

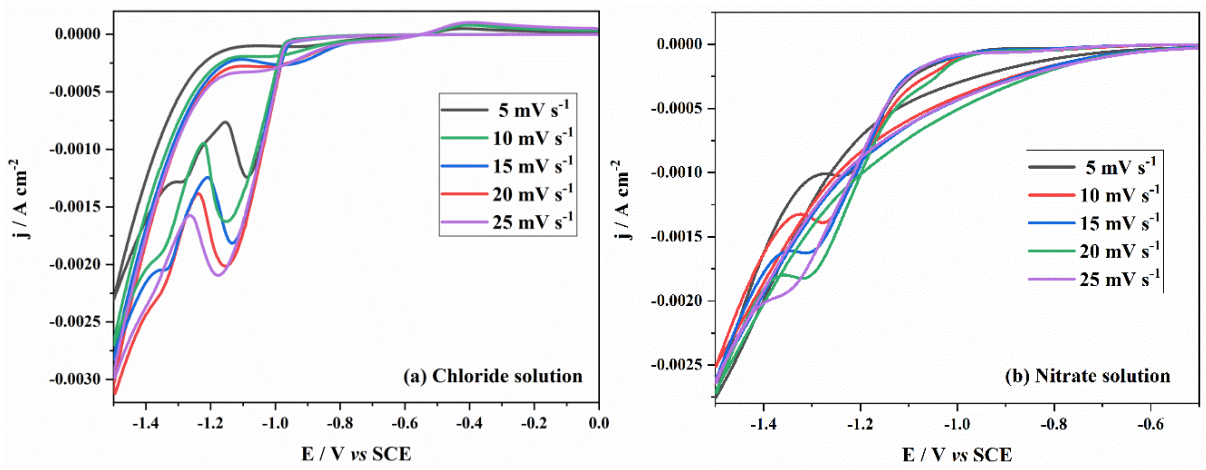

Figure 2. Cyclic voltammograms for Nickel electrodeposition on ITO substrate at different scan rates: (a) from chloride solution, (b) from nitrate solution.

In addition, we noted that the cathodic peaks become more intense upon increasing the scan rate, and are shifted to the negative potentials. Such a shift is typically associated with quasi-reversible electrochemical reactions. The peak currents density j_{peak} are represented as a function of square root of the scan rate ($v^{1/2}$) in **Figure 3,** a good linear relationship with correlation coefficient (R^2=0.99) is obtained indicating the diffusion-controlled process (Bottoni *et al.,* 2023; Lghazi *et al.,* 2021; Lghazi *et al.,* 2018; Grujicic and Pesic 2005).

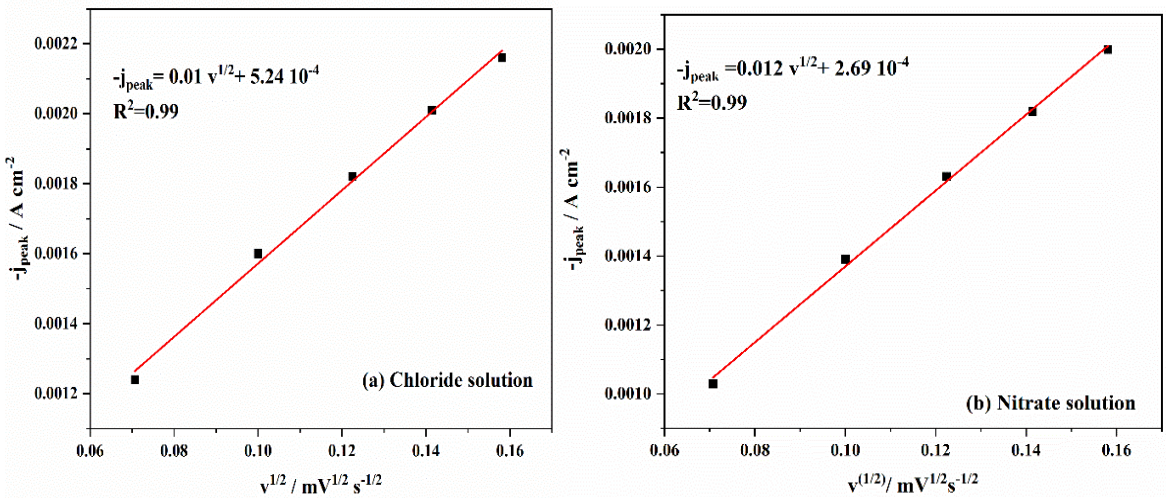

Figure 3. The plot of the cathodic peak current density (j_{peak}) versus the square root of the sweep rate ($v^{1/2}$): (a) in chloride solution and (b) in nitrate solution.

This result is in agreement with other studies carried out on the nickel electrodeposition. Therefore, the Nickel diffusion coefficient in two mediums can be calculated using the equation 9 (Youbi *et al.,* 2020; Aynaou *et al.,* 2022; Wu et al., 2023):

$$-j_{peak} = 367.n^{3/2}.C.D^{1/2}.v^{1/2} \qquad \textbf{(Eqn. 9)}$$

C: is the concentration of species in the bulk of the solution (mol.L^{-1}), j_{peak}: is the peak current density (A.cm^{-2}), n: is the number of electrons, D: is the diffusion coefficient (cm^2.s^{-1}), and v: is the scan rate.

The obtained values of diffusion coefficient in nitrate solution is D=1.01 10^{-6}cm^2.s^{-1} and in chloride solution is D= 1.04 10^{-6}cm^2.s^{-1}. In addition, various information can be extracted from those voltammograms such as cathodic peak and half-peak potentials of nickel reduction for different scan rates, which makes the possibility to investigate the reversibility of this redox system. **Tables 1** and **2** show the values of the peak Epc and half-peak Epc/2 potentials and the calculated difference $|$Epc-Epc/2$|$. This last difference increases as the scan rate increases and the obtained values are higher in all cases than the theoretical value of 2.2RT/zF, which confirms the quasi-reversibility of the system Ni^{2+}/Ni in the two electrolytes (Sharma *et al.,* 2023;Szymczak, 2013; Sandnes *et al.,* 2007).

Table 1. Current density, potential and half-peak potential of cathodic peak as a function of scanning speed deduced from voltammograms in chloride solution (**Figure 2a**).

V (mV/s)	E_{pc} (V/ECS)	J_{pc} (mA cm^{-2})	$\frac{E_{pc}}{2}$ (V/SCE)	$\lvert E_{pc}-\frac{E_{pc}}{2}\rvert$ (V/SCE)
5	-1.09	-1.22	-1.02	**0.07**
10	-1.15	-1.62	-1.04	**0.11**
15	-1.14	-1.82	-1.03	**0.11**
20	-1.15	-2.02	-1.05	**0.10**
25	-1.18	-2.1	-1.04	**0.14**

Table 2. Current density, potential and half-peak potential of cathodic peak as a function of scanning speed deduced from voltammograms in nitrate solution (**Figure 2b**).

V (mV/s)	E_{pc} (V/ECS)	J_{pc} (mA cm^{-2})	$\frac{E_{pc}}{2}$ (V/ECS)	$\lvert E_{pc}-\frac{E_{pc}}{2}\rvert$ (V/SCE)
5	-1.24	-1.03	-1.15	**0.09**
10	-1.28	-1.39	-1.17	**0.11**
15	-1.31	-1.63	-1.19	**0.12**
20	-1.32	-1.82	-1.19	**0.13**
25	-1.38	-1.98	-1.21	**0.14**

3.2. Chronoamperometry

To study the nucleation and growth mechanism of nickel on the ITO substrate from nitrate and chloride electrolytes, the chronoamperometry was used at different deposition potentials. The obtained transient's current density curves are shown in **Figure 4a** and **b**. Two parts can be distinguished in each transient curve. The ascending part corresponds to the formation and growth of nickel nuclei on the substrate which induces that the current density increases rapidly, reaching a maximum j_{max} at a given time t_{max}. With the rising cathodic potential, the maximum current of these transients (j_{max}) increases while the time (t_{max}) decreases because of the increase of the nucleation density with the applied potential. The descending part was attributed to the intervention of a diffusion process. We can conclude that all these current transients are a characteristic response of three-dimensional (3D) multiple nucleation with diffusion-controlled growth.

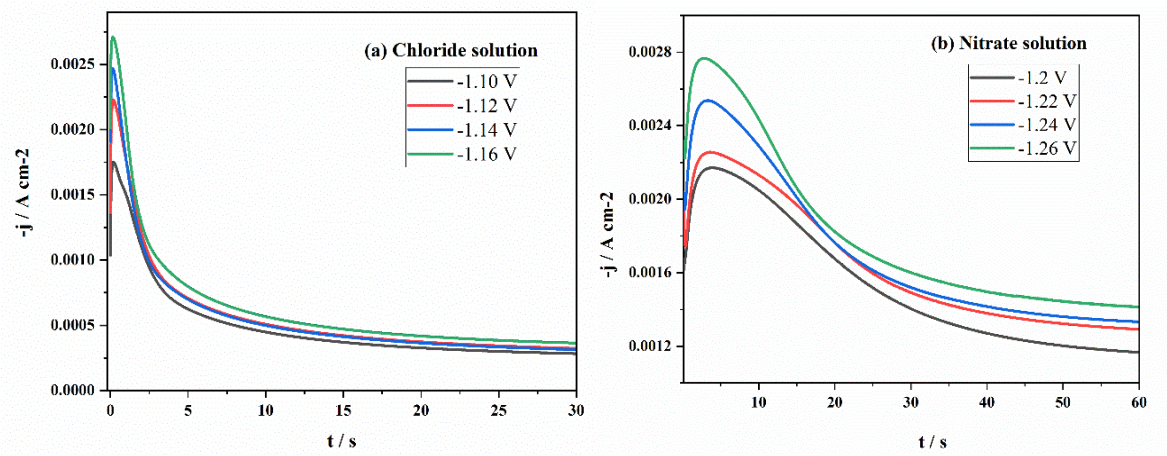

Figure 4. Transients current density for Ni electrodeposition on ITO substrate at different deposition potentials: (a) in chloride solution and (b) in nitrate solution.

To further discuss the nickel electrodeposition mechanism and to identify the type of the process controlling deposition the last part of theses current transits are exploited using Cottrell model (Bahar *et al.*, 2021; Youbi *et al.*, 2020) (**Eqn. 10**) by plotting the $j=f(t^{-1/2})$ evolution in **Figure 5a** and **b** for two case.

$$-j=n.F.C(D/\pi)^{½}\,(t)^{-1/2} \qquad \textbf{(Eqn. 10)}$$

Where nF is the molar charge transferred during electrodeposition, C is the bulk concentration of the electroactive species, D is the diffusion coefficient, and t is time.

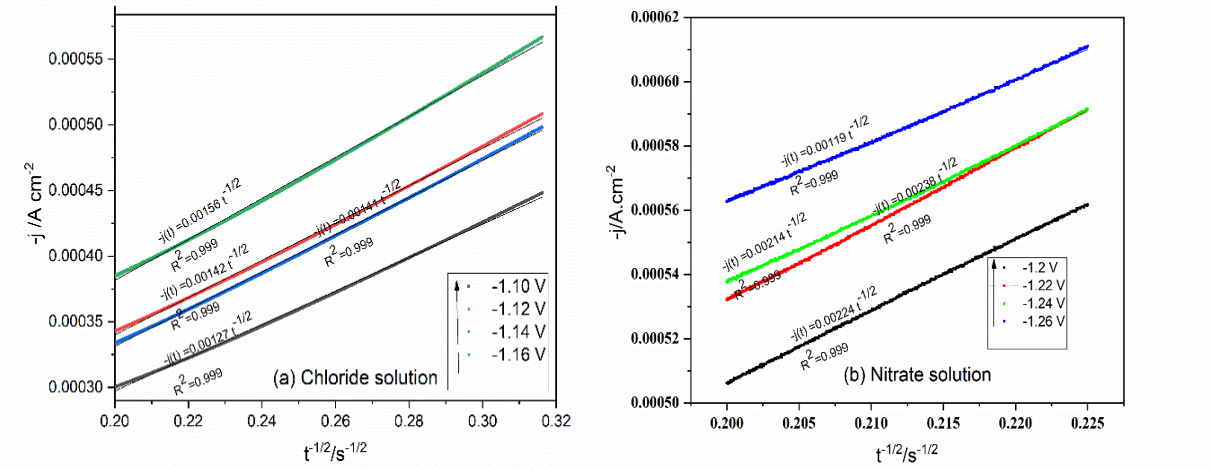

Figure 5. Transients current density (j) versus $t^{-1/2}$ of the last part at different potentials: (a) in chloride solution and (b) in nitrate solution.

These plots show a good linearity between j and $t^{-1/2}$ at different applied potentials, which illustrates the behavior of the redox systems controlled by the diffusion process. It can be concluded that the nickel electrodeposition on ITO substrate in two electrolytic solutions is controlled by the diffusion of the Ni^{2+}. Using the Cottrell equation, the diffusion coefficient values are extracted and illustrated in **Tables 3** and **4**.

Table 3. Diffusion coefficient D of Ni^{2+}in chloride electrolyte at different potentials.

E(V/ECS)	**-1.1**	**-1.12**	**-1.14**	**-1.16**
D($x10^{-6}cm^2.s^{-1}$)	0.16	0.2	0.2	0.23

Table 4. Diffusion coefficient D of Ni^{2+} in nitrate electrolyte at different potentials.

E(V/ECS)	-1.2	-1.22	-1.24	-1.26
D(x10^{-6}cm^2.s^{-1})	0.48	0.54	0.44	0.14

Under this diffusional control, the kinetic theory of electrodeposition makes it possible to describe the mechanism of nucleation and growth using the first part of current transits curves. To further explore the characteristics of the nucleation mode of the first stage of electrodeposition we have drawn j=f($t^{1/2}$) in **Figure 6** and j=f($t^{3/2}$) in **Figure 7** of ascending part of current transients (**Figure 5**), according to the following equations (Mashreghi and Zare 2016; El Haimer *et al.,* 2022):

For instantaneous 3D nucleation $$i = nF\pi \left(2DC\right)^{\frac{3}{2}} \left(M/\rho\right)^{\frac{1}{2}} N_0\, t^{\frac{1}{2}} \qquad \textbf{(Eqn. 11)}$$

For progressive 3D nucleation $$i = \frac{2}{3} nF\pi \left(2DC\right)^{\frac{3}{2}} \left(M/\rho\right)^{\frac{1}{2}} N_0\, A_N t^{\frac{1}{2}} \qquad \textbf{(Eqn. 12)}$$

N_0 is the density of the nuclei, M is the molar mass of the deposit and ρ is the density of the deposit.

As can be seen, the plots of (j)vs($t^{1/2}$) are linear for two mediums, but those of (j)vs($t^{3/2}$) deviates from linearity. This implies that the electrochemical deposition of Ni exhibits instantaneous 3D nucleation. In order to confirm the type of nucleation mechanism, the theoretical Scharifker and Hill models (Himi *et al.,* 2020; Aynaou *et al.,* 2022) was used according to the equations (3) and (4) related to instantaneous and progressive 3D nucleation respectively (Cai *et al.,* 2023; Scharifker and Hills 1983; Gunawardena *et al.,* 1982):

$$\left(\frac{j}{jmax}\right)^2 = 1.9542.\frac{tmax}{t}.\left[1 - e^{-1.2564\frac{t}{tmax}}\right]^2 \qquad \textbf{(Eqn. 13)}$$

$$\left(\frac{j}{jmax}\right)^2 = 1.2254.\frac{tmax}{t}.\left[1 - e^{-2.3367\left(\frac{t}{tmax}\right)^2}\right]^2 \qquad \textbf{(Eqn. 14)}$$

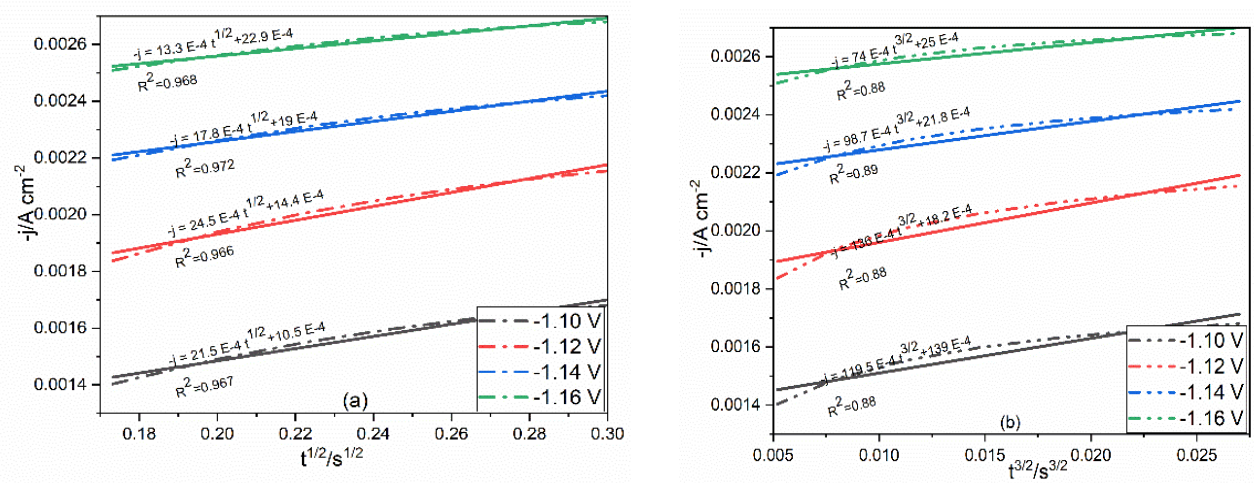

Figure 6. (a)Transients current density (j) versus $t^{1/2}$ of the second part at different potentials and (b) transients current density (j) versus $t^{3/2}$ of the first part at different potentials in chloride solution.

The comparison between the transients of the experimental curves at different potentials during the nickel electrodeposition on ITO substrate, with the theoretical dimensionless transients of j/j_{max} versus $t/_{tmax}$, in **Figure 8** shows that the Ni germs grow according to an instantaneous 3D nucleation mechanism in two mediums (Hu *et al.,* 2023; Bahar *et al.,* 2022; El Haimer *et al.,* 2022).

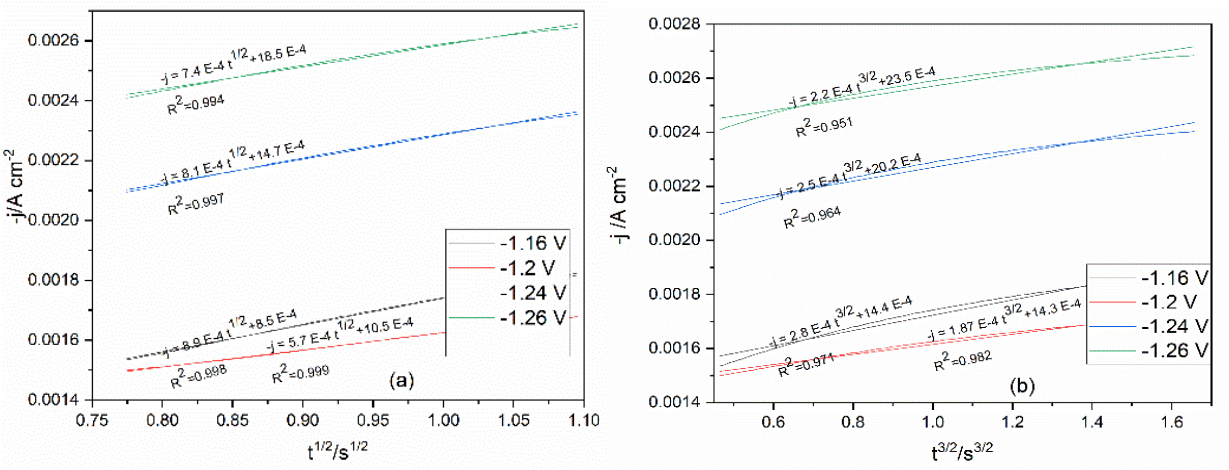

Figure 7. (a)Transients current density (j) versus $t^{1/2}$ of the second part at different potentials and (b) transients current density (j) versus $t^{3/2}$ of the first part at different potentials in nitrate solution.

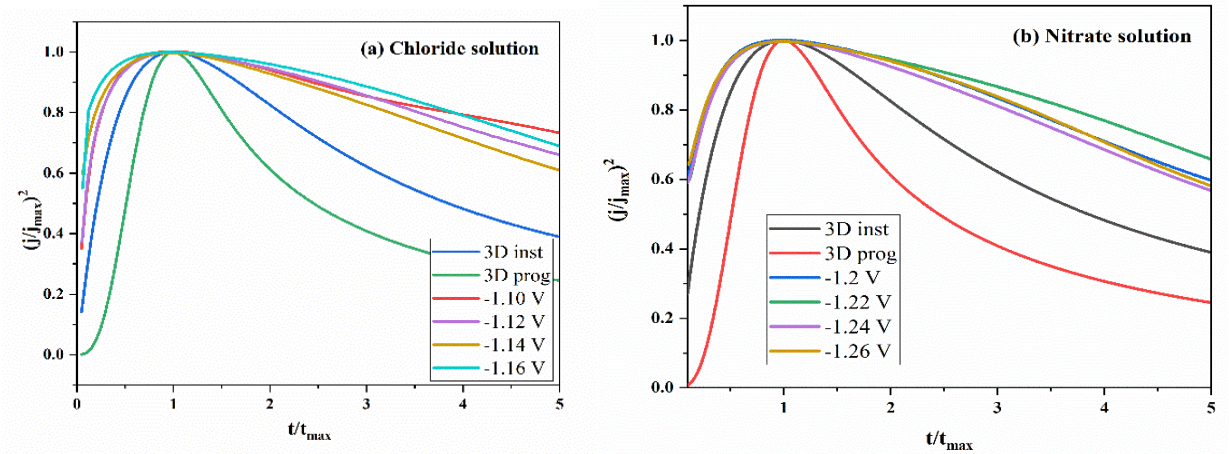

Figure 8. Comparison of theoretical non-dimensional $(j/j_{max})^2$ versus (t/t_{max}) plots for instantaneous and progressive nucleation to experimental transients current density of different potentials. (a) in nitrate solution (b) in chloride solution.

3.3. Characterization

3.3.1. X-ray diffraction (XRD)

The X-ray diffraction patterns of the electrodeposited nickel thin films on ITO substrate at -1.2 V /SCE in nitrate solution, and -1.1 V/ SCE in chloride solution are also investigated. It was found the nickel electrodeposited on ITO substrate has a cubic crystal structure whatever the electrolyte composition (**Figure 9**).

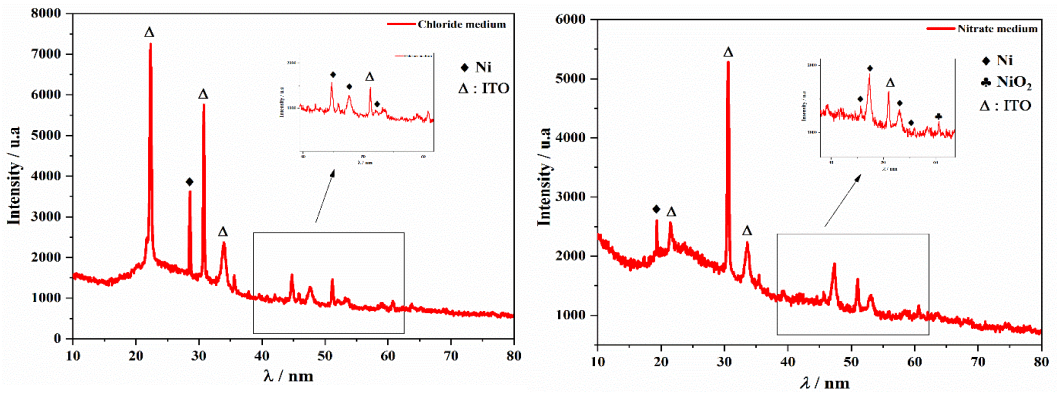

Figure 9. XRD of Ni film deposited on ITO substrate by chronoamperometry: (a) chloride medium and (b) nitrate medium.

The diffractograms of nickel electrodeposited from nitrate and chloride solution present the same peaks. The diffraction peaks at 2θ = 44.833° and 53.045° are characteristic of hexagonal and cubic nickel (Ni) which orientations have been preferred (111) and (200) at two electrolytes (nitrate and chloride). Moreover, in the nitrate medium, new diffraction peaks are observed at 2θ = 61.131° which can be attributed to a new phase that has been formed. According to the literature, these diffraction peaks are characteristic of nickel oxide (NiO_2) whose orientations was preferred (201). These results are in good agreement with those reported in other studies of nickel electrodeposition film. The appearance of some XRD peaks reflections corresponding to ITO substrate.

3.3.2 Scanning electron microscopy (SEM)

Morphological properties of samples nickel thin film are determined and investigated by Scanning Electron Microscopy (SEM) observation. The micrographs of thin films deposited in different mediums (chloride and nitrate) at temperature 25 °C and for 15 min are shown in **Figure 10**. The sample in **Figure 10a** exhibited the only one type of nuclei that correspondent of the Ni.

It can be observed, in this case, that the 3D nucleation takes place at some active sites of the ITO substrate surface and then all nuclei grow three-dimensionally until they collide with each other to form a metallic film. However, the morphological surface shown in **Figure 10b** is completely covered with the uniform nuclei corresponding to the Ni and NiO, this explain that the all-active nucleation sites on the surface are filled.

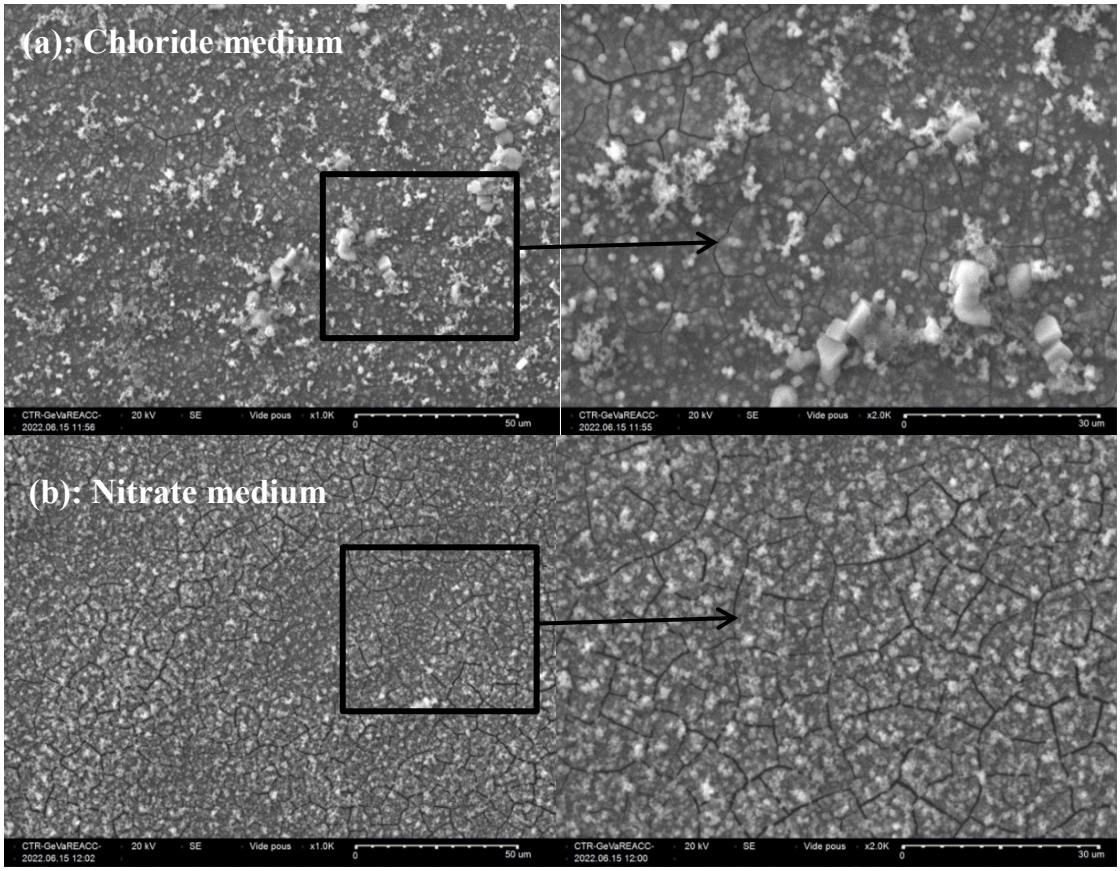

Figure 10. SEM image of Ni electrodeposited on ITO substrate in: (a) Chloride medium, and (b) Nitrate medium.

Conclusion

To sum up, the present work was dedicated to studying the effect of electrolyte composition (nitrate and chloride) on the electrodeposition mechanism of nickel on ITO substrate. First, the cyclic voltammetry and chronoamperometry has shown that the electrodeposition process of nickel from the two mediums is a quasi-reversible reaction controlled by the diffusion. The obtained values of diffusion coefficient in nitrate solution is D=1.01 10^{-6} $cm^2.s^{-1}$ and in chloride solution is D = 1.04 10-6 $cm^2.s^{-1}$. The analysis of chronoamperometric measurements according to Scharifker-Hills model has confirmed that the electrodeposition mechanism of nickel on ITO substrate follows the 3D nucleation instantaneous in the two solutions. In conclusion, we note that the formation of oxide in a nitrate medium makes the chloride electrolyte more preferable to the electrodeposition of nickel on the ITO substrate.

Acknowledgements : The laboratory members of bio-geosciences and materials engineering at the ENS Casablanca are gratefully acknowledged.

Declaration of competing interest : The authors declare no conflicts of interest.

References

Abbasi-Amandi A., Ahmadi N.P., Ojaghi-Ilkhchi M. and Alinezhadfar M. (2021), Physical and electrochemical behavior of black nickel coatings in presence of KNO_3 and imidazole additives. *Journal of Electroanalytical Chemistry,* 893, 115310. https://doi.org/10.1016/j.jelechem.2021.115310

Aynaou A., Youbi B., Himi M.A., Lghazi Y., Bahar J., El Haimer C., Ouedrhiri A. and Bimaghra I. (2022). Electropolymerization investigation of polyaniline films on ITO substrate. *Materials Today: Proceedings,* 66(1), 335-340. https://doi.org/10.1016/j.matpr.2022.05.437

Aynaou A., Youbi B., Lghazi Y., Himi M.A., Bahar J., El Haimer C., Sahlaoui A. and Bimaghra I. (2022), Nucleation, Growth and Electrochemical Performances of Polyaniline Electrodeposited on ITO Substrate. *Journal of the Electrochemical Society,* 169(8), 082509. https://doi.org/10.1149/1945-7111/ac862a

Badea G.E., Dzitac S., Porumb C., Popper L. and Badea T. (2010), Nitrate ion effects on the nickel corrosion and passivation behaviour in 0.5M H_2SO_4 solutions. *Rev. Roum. Chim,* 55(4), 263-267.

Bahar J., Lghazi Y., Youbi B., Ait Himi M. and Bimaghra I. (2021), Comparative study of nucleation and growth mechanism of cobalt electrodeposited on ITO substrate in nitrate and chloride electrolytes. *Journal of Solid State Electrochemistry,* 25(6), 1889-1900. https://doi.org/10.1007/s10008-021-04961-7

Bahar J., Lghazi Y., Youbi B., Himi M.A., El Haimer C., Ouedrhiri A., Aynaou A. and Bimaghra I. (2022), Nucleation and growth mechanism of cuprous oxide electrodeposited on ITO substrate. *Materials Today: Proceedings*. 66, 187-19. https://doi.org/10.1016/j.matpr.2022.04.445

Bottoni L., Darjazi H., Sbrascini L., Staffolani A., Gabrielli S., Pastore G. and Nobili F. (2023), Electrochemical Characterization of Charge Storage at Anodes for Sodium-Ion Batteries Based on Corncob Waste-Derived Hard Carbon and Binder. *ChemElectroChem,* e202201117. https://doi.org/10.1002/celc.202201117

Boumezzourh A., Ouknin M., Bouyanzer A., Costa J. and Majidi L. (2019), *Ammodaucus Leucotrichus* Cosson & Durieu fruits essential oil as corrosion inhibitor of tinplate in 0.5 M oxalic acid medium and its thermodynamic properties. *Moroccan Journal of Chemistry,* 7(1), 141-153. https://doi.org/10.48317/IMIST.PRSM/morjchem-v7i1.14387

Cai H., Li Y., Wu Y., Zhang H., Zhang Y., Sun Y. and Ding G. (2023), Non-Cyanide Thick Silver Electrodeposition Base on Instantaneous Nucleation for 3D Microstructures with High Performance. *Journal of The Electrochemical Society*, 170(2), 022504. https://doi.org/10.1149/1945-7111/acb5c4

Chat-Wilk K., Rudnik E., Włoch G. and Osuch P., (2021), Importance of anions in electrodeposition of nickel from gluconate solutions. *Ionics,* 27(10), 4393-4408. https://doi.org/10.1007/s11581-021-04166-y

Deng M.J., Sun I.W., Chen P.Y., Chang, J.K. and Tsai W.T., (2008), Electrodeposition behavior of nickel in the water-and air-stable 1-ethyl-3-methylimidazolium-dicyanamide room-temperature ionic liquid. *Electrochimica Acta*, 53(19), 5812-5818. https://doi.org/10.1016/j.electacta.2008.03.040

El Haimer C., Lghazi Y., Bahar J., Youbi B., Himi M.A., Aynaou A. and Bimaghra I., (2022), Electrochemical properties of Bi_2Se_3 layers semiconductor elaborated by electrodeposition. *Journal of Electroanalytical Chemistry*, 925, 116906. https://doi.org/10.1016/j.jelechem.2022.116906

El-Hallag I., Elsharkawy S. and Hammad S. (2021). Electrodeposition of Ni nanoparticles from deep eutectic solvent and aqueous solution as electrocatalyst for methanol oxidation in acidic media. *International Journal of Hydrogen Energy,* 46(29), 15442-15453. https://doi.org/10.1016/j.ijhydene.2021.02.049

Grujicic D. and Pesic B. (2005), Reaction and nucleation mechanisms of copper electrodeposition from ammoniacal solutions on vitreous carbon. *Electrochimica Acta,* 50(22), 4426-4443. https://doi.org/10.1016/j.electacta.2005.02.012

Gunawardena G., Hills, G., Montenegro I. and Scharifker B. (1982), Electrochemical nucleation: part I. general considerations. *Journal of Electroanalytical Chemistry and Interfacial Electrochemistry,* 138(2), 225-239. https://doi.org/10.1016/0022-0728(82)85080-8

Himi M.A., Youbi B., Lghazi Y. and Bimaghra I. (2020), Nucleation and growth mechanism of manganese oxide electrodeposited on ITO substrate. *Materials Today: Proceedings,* 30, 963-969. https://doi.org/10.1016/j.matpr.2020.04.358

Hu M., Wang Y., Chen Z., Ning S. and Wei, Y. (2023), Study of Indium electrodeposition and nucleation mechanism in acidic solution using EQCM. *Electrochimica Acta,* 443, 141963. https://doi.org/10.1016/j.electacta.2023.141963

Hu W., Fu, H., Chen L., Wu X., Geng B., Huang Y., Xu Y., Du M., Shan G., Song Y. and Wu Z. (2022), Synthesis of amorphous Nickel-Cobalt hydroxides with high areal capacitance by one-step electrodeposition using polymeric additive. *Chemical Engineering Journal,* 451, 138613. https://doi.org/10.1016/j.cej.2022.138613

Ibrahim M.A. (2006), Black nickel electrodeposition from a modified Watts bath. *Journal of Applied Electrochemistry,* 36(3), 295-301. https://doi.org/10.1007/s10800-005-9077-8

Jamshidi L.C.L.A., Rodbari R.J., Hernandez N., and EP Barbosa C. M. B. M. (2018), Oxidation influence on the quasicrystalline phases of alloys Al62. 5Cu25Fe12. 5 and Al65Ni15Co20. *Moroccan Journal of Chemistry,* 6(3), 6-3. https://doi.org/10.48317/IMIST.PRSM/morjchem-v6i3.5431b

Janjan S.M., Nasirpouri F. and Hosseini M.G. (2011), Electrodeposition mechanism of nickel films on polycrystalline copper from dilute simple sulphate solutions. *Russian Journal of Electrochemistry,* 47(7), 787-792. https://doi.org/10.1134/S1023193511070159

Lghazi Y., Bahar J., Youbi B., Himi M.A., Elhaimer C., Elouadrhiri A., Bimaghra I., Ouknin M. and Majidi L. (2021), Nucleation/Growth and Optical Proprieties of Co-doped ZnO Electrodeposited on ITO Substrate. 12(5), 6776 – 6787. https://doi.org/10.33263/BRIAC125.67766787

Lghazi Y., Bimaghra I., Bachiri A., Elmerzouki K., Youbi B. and Lasri H. (2018), Investigation of the nucleation kinetics of Bi and Δ-Bi_2O_3 during electro-deposition on substrate ITO. *Int. J. Eng. Technol,* 7(4.32), 21-24.

Mashreghi A. and Zare H. (2016), Investigation of nucleation and growth mechanism during electrochemical deposition of nickel on fluorine doped tin oxide substrate. *Current Applied Physics,* 16(5), 599-604. https://doi.org/10.1016/j.cap.2016.03.008

Oluranti S.A., Emmanuel R.S. and Olusesan F.B. (2012), The properties and the effect of operating parameters on nickel plating. *International Journal of Physical Sciences,* 7(3), 349-360. https://doi.org/10.5897/IJPS11.1163

Ritzert N.L. and Moffat, T.P. (2016), Ultramicroelectrode studies of self-terminated nickel electrodeposition and nickel hydroxide formation upon water reduction. *The Journal of Physical Chemistry C,* 120(48), 27478-27489. https://doi.org/10.1021/acs.jpcc.6b10006

Sandnes E., Williams M.E., Bertocci U., Vaudin M.D. and Stafford G.R. (2007), Electrodeposition of bismuth from nitric acid electrolyte. *Electrochimica acta,* 52(21), 6221-6228. https://doi.org/10.1016/j.electacta.2007.04.002

Scharifker B. and Hills G. (1983), Theoretical and experimental studies of multiple nucleation. *Electrochimica acta*, 28(7), 879-889. https://doi.org/10.1016/0013-4686(83)85163-9

Sivasakthi P., Sangaranarayanan M.V. and Prabu H.G. (2021), Micro–nanoarchitectures of electrodeposited Ni–ITO nanocomposites on copper foil as electrocatalysts for the oxygen evolution reaction. *New Journal of Chemistry*, 45(11), 5146-5153. https://doi.org/10.1039/D0NJ05954D

Szymczak J. (2013), Contribution à l'électrodéposition en milieu liquide ionique de tellurure de bismuth en vue de son dopage (Doctoral dissertation, Université de Lorraine).

Wang Y., Li L., Li H. and Wang H. (2019), Electrodeposition of Cu^{2+} in presence of Ni^{2+} in sulfuric acid system. *Ionics*, 25(10), 5045-5056. https://doi.org/10.1007/s11581-019-03037-x

Wu Y., Zhou Z., Yao Q., Wang J., Tian Y., Liu, S. and Wang C. (2023), Electrodeposition nanoarchitectonics of nickel cobalt phosphide films from methyltriphenylphosphonium bromide-ethylene glycol deep eutectic solvent for hydrogen evolution reaction. *Journal of Alloys and Compounds*, 942, 169070. https://doi.org/10.1016/j.jallcom.2023.169070

Youbi, B., Lghazi, Y., El Bachiri A., Himi M.A., Elibrizy O. and Bimaghra I. (2020), Investigation of nucleation and growth mechanism of bismuth electrodeposited on ITO substrate in nitric acid medium. *Materials Today: Proceedings,* 22, 6-11. https://doi.org/10.1016/j.matpr.2019.08.055

Youbi B., Lghazi Y., Himi M.A., Bahar J. and Bimaghra I, (2020), Growth mechanism during the early stages of electrodeposition of bismuth telluride Bi2Te3 on ITO substrate. *Materials Today: Proceedings,* 30, 842-848. https://doi.org/10.1016/j.matpr.2020.04.338

Yue B., Zhu G., ChangZ., Song J., Gao, X., Wang, Y., Guo, N. and Zhai, X. (2022a), Study on surface wettability of nickel coating prepared by electrodeposition combined with chemical etching. *Surface and Coatings Technology*, 444, 128695. https://doi.org/10.1016/j.surfcoat.2022.128695

Yue B., Zhu G., Wang Y., Song J., Chang Z., Guo N. and Xu M., (2022b), Research on wettability of nickel coating changes induced in the electrodeposition process. *Journal of Electroanalytical Chemistry,* 910, 116146. https://doi.org/10.1016/j.jelechem.2022.116146